High-efficiency and flexible photonic microwave harmonic downconverter based on a self-oscillation optical frequency comb

Xin Zhang（张鑫）[1], Tao Pu（蒲涛）[2], Huatao Zhu（朱华涛）[1], Yunshan Zhang（张云山）[3], Gengze Wu（吴庚泽）[2], Jin Li（李晋）[2,*], and Jilin Zheng（郑吉林）[2,**]

[1]College of Information and Communications, National University of Defense Technology, Wuhan, 430010, China
[2]College of Communications Engineering, Army Engineering University of PLA, Nanjing, 210007, China
[3]College of Electronic and Optical Engineering &College of Flexible Electronics (Future Technology), Nanjing University of Posts and Telecommunications, Nanjing, 210023, China
[*]Corresponding author: nj_10120@163.com; [**]Corresponding author: zhengjilinjs@126.com
Received Month X, XXXX; accepted Month X, XXXX; posted online Month X, XXXX

***Abstract*— Photonic microwave harmonic downconverters (PMHDCs) based on self-oscillation optical frequency combs (OFCs) are interesting because of their broad bandwidth compared with plain optoelectronic oscillators. In this paper, a high-efficiency and flexible PHMDC is proposed and demonstrated. The properties of the OFC, such as the carrier-to-noise ratio (CNR), bandwidth, free spectral range (FSR) and the influence of optical injection are investigated. The broadband OFC provides a frequency tunable and high-quality local oscillation (LO), which guarantees flexible down conversion for the RF signal. The sideband selective amplification (SSA) effect not only improves the conversion efficiency, but also promotes single-sideband modulation. The conversion range can reach 100 GHz. The 12-40 GHz RF signal can be downconverted to IF signals with a high conversion efficiency of 14.9 dB. The fixed 40-GHz RF signal is flexibly down converted to IF signal with the frequency from 55.4 MHz to 2129.4 MHz. The phase noise of IF signal at a frequency offset of 10-kHz is the same as that of the input RF signal. The PMHDC shows great performance and will find applications in RoF, electronic warfare receivers, avionics, and wireless communication systems.**

***Key words*—frequency down-conversion, optical frequency comb, optical injection, optoelectronic oscillation.**

1. INTRODUCTION

The microwave downconverter provides an effective way to meet the urgent demand for processing and receiving ultrahigh frequency signals with the development of 5G, millimeter wave communication, modern electronic warfare receivers, the internet of things and other emerging technologies [1-3]. Electrical mixers are employed in conventional microwave systems to realize frequency down conversion, which suffers from small bandwidth, poor isolation, weak anti-electromagnetic interference, and high nonlinear effect. To solve these problems, the photonic microwave downconverters (PMDCs) have been proposed [4-14], which has infinite isolation between the microwave input and the local oscillator. In the optical domain, the PMDC is realized through three key steps: 1) The radiofrequency (RF) is converted to an optical signal. 2) The optical signal for local oscillation (LO) is generated. 3) The intermediate frequency (IF) is generated by beating the LO and RF optical microwave signals by a low-speed photodetector (PD). Usually, to avoid the narrow bandwidth of direct modulation, the LO is modulated to the optical carrier by using a dual-parallel Mach-Zehnder modulator [4] and cascaded or parallel electro-optic modulators [5-7]. At the same time, researchers are committed to improving the conversion efficiency [8-10], e.g., the conversion efficiency can reach 11.3 dB based on the stimulated Brillouin scattering loss spectrum to suppress the optical carrier [8].

Recently, the optoelectronic characteristics of semiconductor lasers have received extensive attention for photonics microwave mixing. The optical injection (OI) technique is applied in PMDCs to improve the direct modulation bandwidth, with sideband injection locking [11] or harmonic injection locking [12] based on the period-one oscillation. To further improve the operation bandwidth, a photonic microwave harmonic downconverter (PMHDC) has been proposed based on the optical frequency comb (OFC), which provides high-frequency harmonics [13,14]. In [13], the 75-110 GHz RF signal is down converted. Except for that based on cascaded modulators and semiconductor optical amplifiers, the OFC can be generated by the gain-switching effect, with the advantages of easy implementation, robustness, and stability [15,16]. The LO is essential in the above systems, its quality will affect the phase noise of IF signal. Due to the structure of optoelectronic oscillation (OEO), the microwave signal with ultralow phase noise and high frequency is obtained, which avoids the use of LO signal [17-19]. To obtain a broader bandwidth, self-oscillation OFCs have been proposed [20-22], which are expected to be applied in PMHDCs. However, external modulators are still employed to generate OFCs, which increases the cost.

In this paper, a high-efficiency and flexible PMHDC based on a self-oscillation OFC is proposed and experimentally demonstrated. The high efficiency benefits from the sideband selective amplification (SSA) effect based on OI, which forms single sideband modulation by amplifying one sideband. The flexibility of down conversion benefits from the self-oscillation OFC with tunable free spectral range (FSR), which provides high-quality and tunable LO, avoiding external LO and modulators. In addition, the PMHDC has a

broad operation bandwidth up to 100 GHz owing to OI. The LO is obtained by a self-oscillation OFC based on the optoelectronic oscillation at the relaxation oscillation (RO) frequency. The Δf_{10}, which is defined as the 10-dB spectra width, reaches 101.34 GHz, representing an improvement of approximately 50 GHz compared with that without OI. The influence of the injection strength as well as the detuning frequency between the master and slave laser on the OFC are investigated. With harmonic down conversion, the 12-40 GHz RF signals are converted to IF signals below 3 GHz when the FSR is 5.6895 GHz. The conversion efficiency reaches as high as 14.9 dB. By changing the FSR, the same 40-GHz RF signal can be converted to IF signals with frequencies ranging from 55.4 to 2129.4 MHz. The phase noise of the IF signal only deteriorates at high frequency offset compared with the RF signal owing to the high performance of the self-oscillation OFC. Other parameters, such as spurious free dynamic range (SFDR) and performance for down conversion of high-frequency vector signals, are investigated, indicating that the system is competent for down conversion applications.

2. Principle And Experimental Setup

Figure 1 illustrates the experimental diagram of proposed photonic microwave harmonic downconverter. The optical carrier f_{ML} of master laser (ML) is equally split into two branches (A and B). In the upper branch, the ML wave is injected into the distributed feedback (DFB) laser, which is marked as SL1. Then, 50% of the optical signal is sent to opto-electronic oscillation loop, as introduced in previous work [23]. In the other branch, the RF signal with a frequency of f_{RF} is modulated to ML wave through the phase modulator (PM, EOSPACE: PM-DV5-40-PFU-PFU-LV) with a bandwidth of 40 GHz. Then, the optical signal with double sidebands is injected into the DFB laser marked as SL2. Finally, the optical signal coupled from the two branches is sent to the wavelength selective switcher (WSS, Finisar: 10WSAA09FLL). After amplified by the erbium-doped fiber amplifier (EDFA, EDFA-BA15-APC), the signal is converted to an electrical signal by PD (TELEDYNE LECROY OE6250G-M) with a maximum input power of 9 dBm. The polarization controllers (PCs) are used to adjust the polarization of the ML to align it with that of the SL1/2 to maximize the injection efficiency. The optical attenuators (ATTs) are used to adjust the optical power.

The realization of a high-efficiency and flexible PMHDC is shown in Fig. 1(b). In the OFCG part, an OFC with a tunable FSR and high carrier-to-noise (CNR) can be obtained based on the OEO [23]. Then, turn on the ML and adjust the wavelength f_{ML} close to one comb of the OFC. The whole OFC will be locked to the ML mode after OI. The ML mode is consequently coherent with all the combs of the OFC. In the part of SSA, the single sideband (SSB) signal is obtained. At the output of the PM, the double sideband signal with low-power sidebands is generated. After OI, the free-running SL2 mode f_{SL2} will red-shift to f'_{SL2} with a surrounding gain spectrum [24]. If the -1st sideband falls into the gain spectrum, it will be amplified. The SSB signal with a high-power sideband is obtained. At the same time, the amplified -1st sideband is coherent with the ML mode. Consequently, it is coherent with the combs of the OFC. The -1st sideband as well as one comb f_{ML}-nf_{RO}, which is n^{th} FSR apart from the ML mode, are filtered out by the WSS. Thus, the down-converted IF signal at $f_{IF}=|f_{RF}-nf_{RO}|$ can be generated. The high-efficiency downconverter benefits from the SSA effect. Without the SSA effect, the power of the -1st sideband is low. So, the high carrier-to-sideband ratio results in the low power for the beating frequency. The highest power for the down-converted signal can be obtained when carrier-to-sideband ratio is 0 dB with the SSA effect.

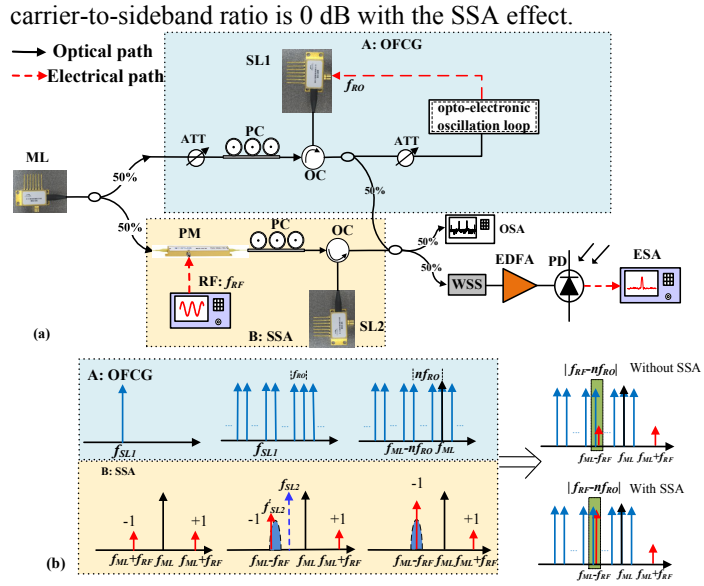

Fig. 1. (a) Schematic diagram of the proposed photonic microwave harmonic downconverter. (OFCG: optical frequency comb generator, SSA: sideband selective amplification, ML: master laser, PC: polarization controller, OC: optical circulator, SL1/2: slave laser 1/2, ATT: optical attenuator, PD: photodetector, PM: optical phase modulator, WSS: wavelength selective switcher, EDFA: erbium-doped fiber amplifier, OSA: optical spectrum analyzer, ESA: electrical spectrum analyzer). (b) Illustration of the high-efficiency PMHDC based on self-oscillation OFC and SSA effect.

3. Results And Discussion

This section is divided into three aspects: ⅰ) Harmonic injection locked OFC with OI. ⅱ) SSA effect under optical injection locking. ⅲ) High-efficiency PMHDC based on the self-oscillation OFC and SSA effect. For the OFC, characteristics such as the Δf_{10} and CNR are measured, and the influence of OI is also investigated to obtain the optimized OFC. For the PMHDC, parameters such as conversion efficiency, frequency tunability, SFDR and quality of the IF signal are measured.

A. *Improvement of the OFC characteristics with OI*

The OFC can be obtained based on directly modulated OEO [23]. However, the CNR will be degraded if the feedback power is high as the blue line in Fig.2(a). OI will improve the performance of the OFC based on the gain-switching effect [16]. Keep the SL1 parameters unchanged. After setting the ML mode at 1548.23 nm and the output power at 3.5 dBm, the beating frequency between ML and SL1 is 37.71 GHz when the loop is open. Keeping the feedback optical power unchanged at 3 dBm, the noisy OFC will re-evolve into a high-quality OFC, as shown by the red curve in Fig. 2(a). The CNR is 35 dB, and there are 14 combs within a 10 dB power

fluctuation, indicating a Δf_{10} of 73.19 GHz. The corresponding electrical spectra are shown in Fig. 2(b). The details for the fundamental frequency are plotted in Fig. 2(c) with the sidemode suppression ratio of 59 dB. The performance of phase noise is greatly improved compared that without injection under the condition of high-power feedback. The influence of the OI strength on the performance of the OFC is also investigated. With increasing injection strength from -20.5 dBm to 3.5 dBm, the CNR increases from 3 dB to 35 dB as Fig. 3 shows. With OI, a clear OFC based on the ML mode appears above the noisy spectral envelope. With increasing injection power, in the competition between the spontaneous emission and the injected field to build up the emitted pulses, the ML mode will be in an increasingly dominant position, and the pulses will be locked to the external injection.

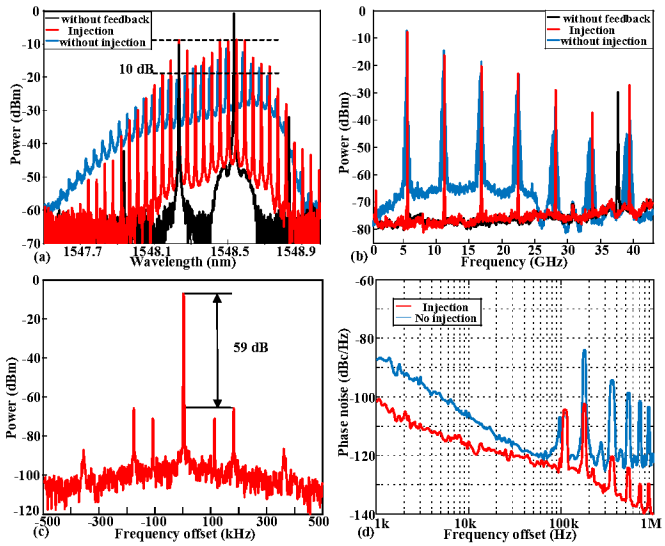

Fig. 2. (a) Optical spectra for the generated OFC under different conditions. (b) Corresponding electrical spectra. (c) The electrical spectrum of the signal at 5.63 GHz. (d) The phase noise of the signal at 5.63 GHz with/without OI.

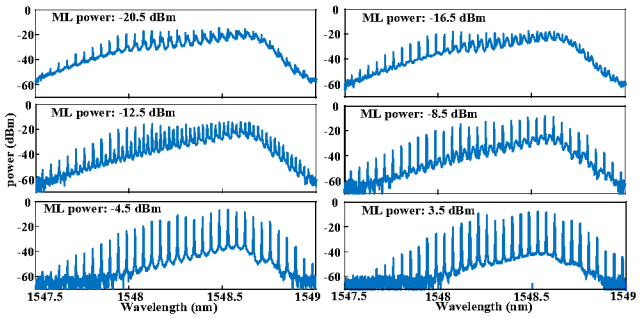

Fig. 3. OFCs generated for a varying OI strength.

Except for the injection strength, the influence of the detuning frequency between the ML and SL1 modes on the OFC performance is researched. With the same low injection power, the quality of the poor OFC can be improved by moving the wavelength of the ML close to one of the peaks of the poor OFC. If the ML power is set at -10.5 dBm and the ML wavelength is still 1548.23 nm, the OFC is remains poor, as the red curve shown in Fig. 4. Not all pulses are locked, resulting in a poor CNR of 7.25 dB. However, keeping the ML power unchanged and tuning the wavelength by -0.012 nm, leads to a high-quality OFC with CNR of 26.4 dB. Compared with the wavelength at 1548.23 nm shown in Fig. 3, the injection power required to reach locking condition is 6 dB lower. The locking range is related to the injection power. With increasing injection power, the locking range will be further expanded. Set the ML power at 3 dBm and adjust the ML wavelength from -0.04 nm to 0.04 nm in steps of 0.02 nm, the corresponding OFCs are shown in Fig. 5. After locking, the CNR is high, and the change in the OFC spectrum follows the ML mode, which proves that the pulses are locked to the ML.

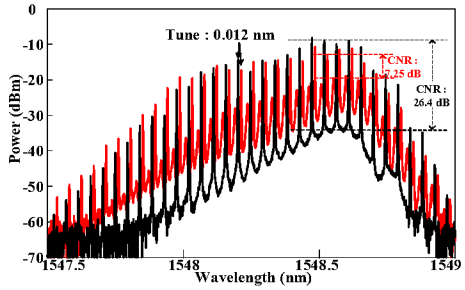

Fig. 4. OFCs generated for a varying ML wavelength at the same power of -10.5 dBm.

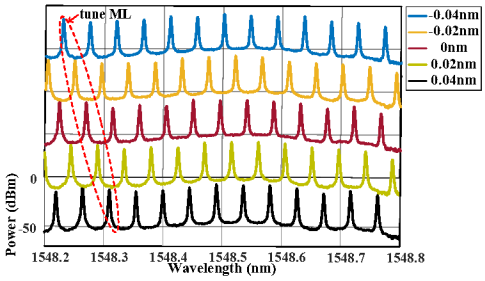

Fig. 5. The change in the OFCs when the wavelength of ML is adjusted in the locking condition.

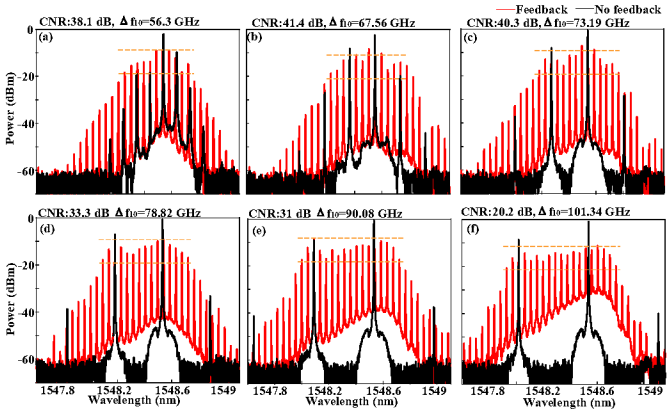

Fig. 6. Generation of the 2~12th harmonic locked OFC.

When the injected ML mode is close to one harmonic of the directly modulated OFC, the OFC will be locked to the ML, and the combs of the OFC are all coherent with the ML mode. The characteristics of the OFCs for a ML power of 2 dBm and adjustment of the ML wavelength to lock the 2~12th harmonic are measured, as shown in Fig. 6. The black curves are the optically injected spectra with no optoelectronic feedback, and the red curves are the evolution of the OFCs. When the higher order harmonic is locked, Δf_{10} is enlarged from 50.67 GHz to 101.34 GHz, which indicates that more flat combs are generated. It should be noted that this will also lead to degradation of CNR, and the quality of the corresponding

electrical signal will be slightly reduced. Increasing the ML power to achieve completely harmonic locking will solve the problem. The high harmonic injection locking technique provides an effective method to broaden the OFC bandwidth. On the other hand, it will permit higher frequency signals to be down-converted, as described in the next section. There is no need to use high-frequency modulators, electrical amplifiers, and PDs to realize this function.

B. Sideband selective amplification (SSA) effect of optical injection locking

In the lower branch, the RF signal is modulated to the ML wave by the phase modulator. Benefitting from the SSA effect, the SSB modulation is realized to avoid the influence of double sideband modulation. After injected into SL2, the -1st sideband is amplified based on optical injection locking. In the experiment, the wavelength of free-running SL2 is 1548.18 nm, as shown by the black curve in Fig. 7. After OI, SL2 will redshift, and a gain spectrum is observed (red curve) [24,25]. The frequency spacing between the ML and the gain spectrum is set to approximately 40 GHz. The 40-GHz RF signal with a power of -25 dBm is modulated to ML. Based on the SSA effect, the -1st sideband falls into the gain spectrum and is amplified by 26.62 dB compared with the +1st sideband, which will improve the power of the output IF signal. Thus, a high-efficiency PMHDC can be obtained. The frequency spacing can be tuned by adjusting the injection ratio and detuning frequency between ML and SL2. Fig.7(b) shows the optical spectrum of injection locking state when the frequency spacing is 100/190 GHz, which satisfies the bandwidth of the OFC and high-frequency microwave signal is permitted to be down-converted.

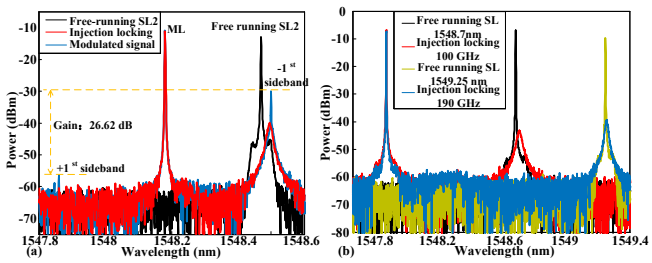

Fig. 7. (a) The output optical spectra for SL2: free-running SL2 with no OI (black), injection locking state with a gain spectrum (red); when the RF signal is modulated to the ML (blue). (b) Optical spectra with different frequency spacings of 100 GHz and 190 GHz.

C. Demonstration of PMHDC with High Efficiency and Flexibility

The high-efficiency and flexible photonic microwave harmonic downconverter with broad bandwidth is realized based on the optically injected self-oscillation OFC and SSA effect. The ML wavelength is set at 1548.28 nm. In the OFCG branch, the FSR of the OFC is set at 5.6895 GHz, and the corresponding 7 times of FSR is 39.826 GHz. In the SSA branch, a 38-GHz RF signal with a power of -25 dBm is modulated to the PM. The frequency spacing between the ML and the gain spectrum is approximately 38 GHz. The combined output optical signal is shown in Fig. 8(a). With the SSA effect, the -1st sideband is amplified 23.04 dB compared with the +1st sideband. The 7th harmonic comb and the amplified -1st sideband are filtered out by the WSS and amplified by the EDFA. The output optical power is 8.65 dBm before PD, and the corresponding IF signal power is -10.81 dBm with the frequency of 1.8269 GHz, which is 14.19 dB higher than that of the RF source, as shown in Fig. 8(b). On the other hand, the power of the IF signal is only -49.1 dBm when the SL2 current is just below the threshold for light emission. This means that the SSA effect provides a gain of 38.29 dB for the IF signal. Overall, the conversion efficiency of the system reaches 14.19 dB.

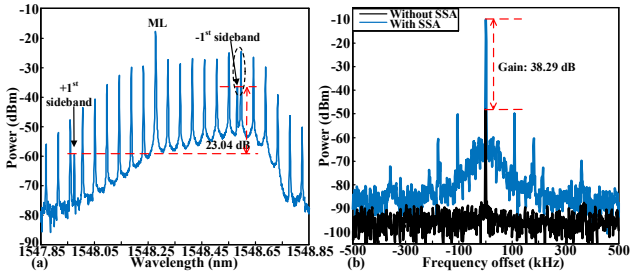

Fig. 8. (a) The optical spectra for the combined output. (b) The electrical spectra for the downconverted signal with/without the SSA effect.

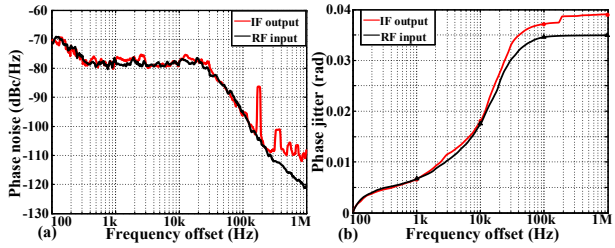

Fig. 9. (a) Phase noise of the input RF signal and output IF signal. (b) The corresponding phase jitter of the signals.

Next, the phase noise performance of the IF signal is analyzed. The SSB phase noise spectra for the input RF signal and output IF signal are measured, as shown in Fig. 9(a). Compared with the 38-GHz input RF signal, the IF signal shows a similar phase noise performance at the frequency offset below 100 kHz. Several peaks are observed above 100 kHz, which are attributed to the sidemodes of the self-oscillation signal, shown in Fig. 2(c). Fig. 9(b) illustrates the phase jitter integrated from 100 Hz to 1 MHz. Generally, the phase noise of the output IF signal is determined by the SSA effect and the self-oscillation signal of the OFC, which shows great phase noise performance owing to the optoelectronic oscillation.

Then, the ability to convert RF signals with different frequencies is investigated. The frequency of the RF signal is changed from 40 GHz to 11 GHz, and the parameters for SL2, such as power and wavelength, are adjusted to tune the gain spectrum accordingly. The optical spectra are shown in Fig. 10(a). The IF signal will be generated by beating the -1st sideband and the comb that is closest to the -1st sideband. Therefore, the frequency of the IF signal is limited below half of FSR. The corresponding IF signal is measured and shown in Fig. 10(b). The information bar on the right shows the corresponding relationship between RF and IF. The conversion efficiency of the RF signal with different frequencies is measured and plotted in Fig. 10(c). The maximum conversion efficiency can reach 14.9 dB. It rolls down to 9.05 dB when the RF frequency is 11 GHz. Because the ML power is decreased to -6.4 dBm to obtain the injection

locking state, the power of the -1st sideband will be decreased accordingly. On the other hand, due to the expansion of the OFC bandwidth with high-order harmonic injection, as shown in Fig. 6(f), RF signals with higher frequencies up to 100 GHz can be effectively downconverted to the IF signal based on the system, which greatly reduces the requirements for receivers.

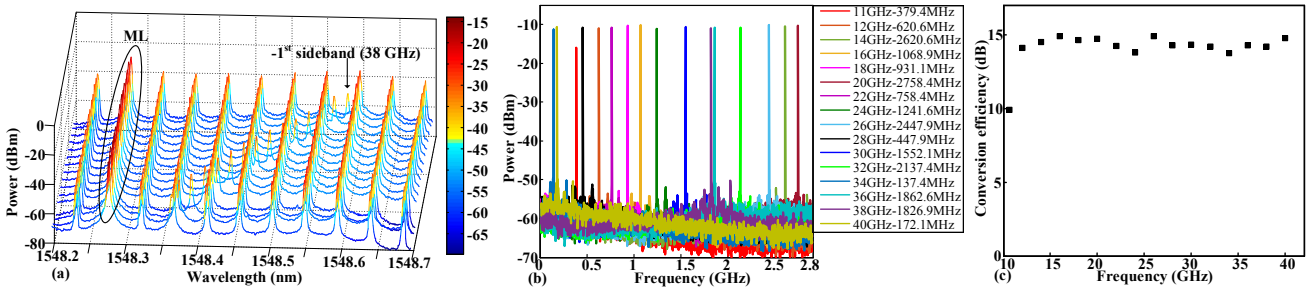

Fig. 10. (a) The optical spectra when the frequency of the input RF signal is varied from 11 GHz to 40 GHz. (b) The electrical spectra for the corresponding IF signals. (c) The conversion efficiency of the system for RF signals with different frequencies.

Moreover, the tunability of converting the fixed RF signal to different IF signals is important, which can be realized based on the OFC with a flexible FSR. By adjusting parameters such as the bias current and wavelength of ML/SL1, the FSR can be tuned from 4.7897 to 6.9725 GHz. Thus, the 40-GHz RF signal can be down-converted to an IF signal with a frequency from 55.4 to 2129.4 MHz, as shown in Fig. 11. The results indicate that the system shows not only a high conversion efficiency but also flexibility of frequency conversion, which can meet the requirements for different scenarios.

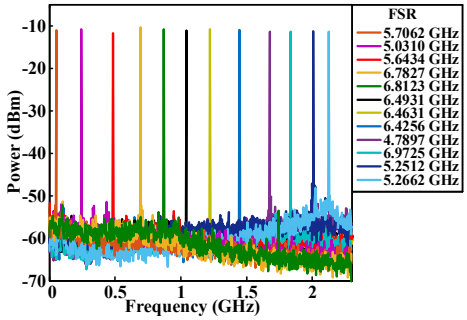

Fig. 11. The corresponding IF signals with high conversion efficiency are obtained when adjusting the FSR.

The SFDR is another important parameter for the frequency down-conversion system, which is experimentally investigated by conducting a two-tone measurement. f_{RF1}=20 GHz and f_{RF2}=19.99 GHz (generated from Agilent N5183A: 100 kHz-20 GHz) with an output power of -36 dBm are injected into the system. The frequency of local oscillation f_{LO} = 4×FSR = 22.758 GHz. The frequencies of the corresponding IF signals are f_{IF1}=2758 MHz and f_{IF2}=2768 MHz. The electrical spectra for the IF signals are shown Fig. 12(a). In addition to the fundamental signals, third-order intermodulation distortion (IMD3) signals appear at $2f_{IF1} - f_{IF2}$ = 2748 MHz and $2f_{IF2} - f_{IF1}$= 2778 MHz. The RBW for ESA is set at 1 kHz, and the noise floor is -79 dBm. Therefore, the noise floor is -79-10×log(1k) =-109 dBm when RBW=1 Hz. The input power of RF1 and RF2 is adjusted to measure the output power of the downconverted fundamental and IMD3 signals. The results are plotted in Fig. 12(b). The SFDR of the system is 84.7 dB·Hz$^{2/3}$. The laser used in the experiment has a linewidth of several MHz. If a narrower linewidth laser source is employed, the SFDR and the conversion efficiency can be improved.

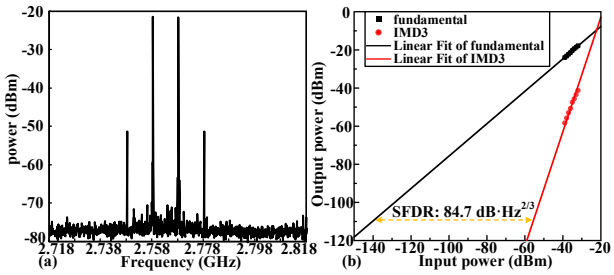

Fig. 12. (a) The electrical spectra measured for the IF signals. (span=1 MHz, RBW=1 kHz). (b) Measured fundamental and IMD3 components as a function of the input RF signal power.

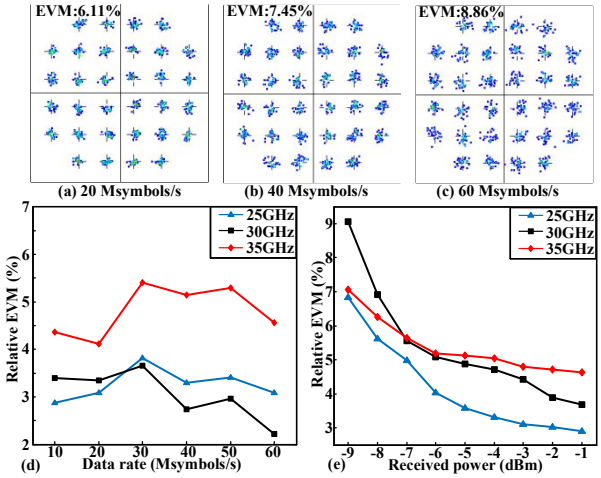

Fig. 13. (a)-(c) The constellation of the IF signal with different data rates. (d) The EVMs for the IF signals when the data rate and carrier frequency are different. (e). The change in the EVM and SNR with output optical power.

Finally, the performance for down-conversion of the high-frequency vector signal is investigated. The high-frequency vector signal (30 GHz with 32 QAM signal) is generated by mixing a low-frequency vector signal (generated by R&S SMBV100A, 5 GHz with 32 QAM signal) with a microwave signal (25 GHz). Figures 13(a)-(c) show the constellation of the IF signal for 32QAM signal with data rates of 20/40/60 Msymbols/s, respectively. The constellation of the signal is clear. The error vector magnitudes (EVMs), as one of the key indicators to characterize the quality of the system for receiving modulated signals, are measured. The EVM increases as the rate increases because the quality of the high-frequency vector source gradually deteriorates. The relative EVM, which indicates the influence of the system on

the source, is calculated and plotted in Fig. 13(d) when the rate and carrier frequency of 32QAM signal are different. The relative EVMs are all lower than 6%, which indicates that the system has little influence on the vector signal. Moreover, the variation in the EVM and signal-to-noise ratio (SNR) with the received optical power are measured and plotted in Fig. 13(e). With increasing optical power from -9 dBm, the EVM decreases from 9.56% and the SNR increases from 20.72 dB. The EVMs for all these converted signals are less than 10%, which satisfies the technical requirement of the satellite communication system.

4. Conclusion

A PMHDC is experimentally realized based on a self-oscillation OFC and the SSA effect. Owing to optical injection, the OFC has a broad bandwidth and flexible FSR, which provides a high-frequency, high-quality and tunable LO for downconversion. The external LO and optical modulators are avoided. Owing to the SSA effect, a high-efficiency IF is obtained by beating the amplified -1st sideband and optical LO. The parameters for the OFC, such as CNR, FSR, and Δf_{10}, are measured, and the influence of optical injection such as the injection ratio and detuning frequency on the OFC is also investigated. The SSA effect can provide gain for the RF signal with the frequency varying from 10 GHz to 190 GHz. RF signals with frequencies of 12-40 GHz are converted to IF signals below 3 GHz with a conversion efficiency above 14 dB. By tuning the FSR, the 40-GHz RF is converted to IF signals with frequency from 55.4 to 2129.4 MHz. The SFDR and great performance of the PMHDC system for converting high-frequency vector signals indicate that it has potential for broad applications in satellite communication systems, RoF, electronic warfare receivers, avionics, and wireless communication systems.

Acknowledgement

This work was supported in part by National Natural Science Foundation of China (62071487, 62201615, 62301569, 62371470).

References

[1] X. Cao, J. Du, G. Ji, D. Zhou, Y. Cheng, M. Li, N. Zhu and W. Li, "Filter-free photonic picrowave I/Q modulator for reconfigurable frequency mixing," J. Lightw. Technol., **41,** 2707 (2023).

[2] C. Browning, E. P. Martin, A. Farhang and L.P. Barry, "60 GHz 5G radio-over-fiber using UF-OFDM with optical heterodyning". IEEE Photon. Technol. Lett. **29,** 2059 (2017).

[3] L. McKay, C. Lai, N. J. Athanasios, D. Y. Choi, S. J. Madden, B. J. Eggleton, and M. Merklein, "Chip-based SBS for image rejection in a broadband microwave photonic mixer". Opt. Express. **31**, 4268 (2023).

[4] D. Chen and J. Ma. "Microwave photonic up- and down-converter with tunable phase shift based on an integrated dual-polarization dual-parallel Mach-Zehnder modulator without optically filtering". Fiber and Integrated Optics **39**, 97 (2020).

[5] G. K. Gopalakrishnan, R.P. Moeller, M.M. Howerton, "A low-loss downconverting analog fiber-optic link". IEEE Transactions on Microwave Theory and Techniques **43**, 2318 (1995).

[6] E. H. W. Chan and R. A. Minasian, "Microwave photonic downconverter with high conversion efficiency". J. Lightw. Technol., **30**, 3580 (2012).

[7] R. Vincent, Pagán, M. Bryan, Haas, and T. E. Murphy, "Linearized electrooptic microwave downconversion using phase modulation and optical filtering". Opt. Express. **19**, 883 (2011).

[8] E. H. W. Chan and R. A. Minasian. "High conversion efficiency microwave photonic mixer based on stimulated Brillouin scattering carrier suppression technique". Opt. Lett. **38**, 5292 (2013).

[9] P. Li, W. Pan, X. Zou, S. Pan, B. Luo and L. Yan, "High-efficiency photonic microwave downconversion with full-frequency-range coverage," IEEE Photonics J., **7**, 5500907 (2015).

[10] T. Zhang, F. Zhang, X. Chen and S. Pan, "A simple microwave photonic downconverter with high conversion efficiency based on a polarization modulator". in Asia Communications and Photonics Conference. Shanghai, China, paper AF2E.4. Nov. (2014).

[11] Y. Hung and S. Hwang, "A novel photonic microwave down-converter based on period-one dynamics of semiconductor lasers". In 2017 Opto-Electronics and Communications Conference (OECC) and Photonics Global Conference (PGC), Singapore, pp. 1-3, Nov (2017).

[12] P. Zhou, N. Li, and S. Pan, "Photonic microwave harmonic down-converter based on stabilized period-one nonlinear dynamics of semiconductor lasers". Opt. Lett. **44**, 4869 (2019).

[13] Y. Zhao, X. Pang, L. Deng, X. Yu, X. Zheng, and I. F. Monroy, "Ultra-broadband photonic harmonic mixer based on optical comb generation". IEEE Photon. Technol. Lett., **24**, 16 (2012).

[14] X. Zou, S. Zhang, H. Wang, Z. Zhang and Y. Liu, "Microwave photonic harmonic down-conversion based on cascaded four-wave mixing in a semiconductor optical amplifier," IEEE Photon. J. **10**, 5500308 (2018).

[15] A. Rosado, M. R. Fernández-Ruiz, P. Corredera, J. M. G. Tijero and I. Esquivías, "High-density and broad band optical frequency combs generated by pseudo-random phase modulation of optically injected gain-switched semiconductor lasers," Optics & Laser Technology, **163**, 109312 (2023).

[16] A. Rosado, R. Antonio, J. Tijero, A. Valle, L. Pesquera and I. Esquivias, "Numerical and experimental analysis of optical frequency comb generation in gain-switched semiconductor lasers", IEEE J. Quantum Electron., **55**, 2001012 (2019).

[17] D. Zhu, S. Pan, S. Cai, and D. Ben, "High-performance photonic microwave downconverter based on a frequency-doubling optoelectronic oscillator". J. Lightw. Technol. **30**, 3036 (2012).

[18] X. Fan, J. Du, G. Li, M. Li, N. Zhu and W. Li, "RF self-Interference cancellation and frequency downconversion with immunity to power fading based on optoelectronic oscillation," J. Lightw. Technol., **40**, 3614 (2022).

[19] Y. Ma, Z. Zhang, J. Yuan, Z. Zeng, S. Zhang, Y. Zhang, Z. Zhang, D. Fu, J. Wang and Y. Liu, "Optically tunable microwave frequency downconversion based on an optoelectronic oscillator employing a phase-shifted fiber Bragg grating". IEEE Photon. J. **10**, 5501611 (2018).

[20] Y. Cheng, J. Yan, and S. Zhao, "Self-oscillating parametric optical frequency comb generation using an electro-absorption modulated laser-based optoelectronic oscillator," IEEE Photon. J., **11**, 5502309 (2019).

[21] R. Ullah, S. Ullah, G. Z. Khan, Y. Mao and J. Khan, "Ultrawide and tunable self-oscillating optical frequency comb generator based on an optoelectronic oscillator". Results in Physics, **22**, 103849 (2021).

[22] J. Yan and A. Liang. "Self-oscillating frequency comb generation with a stimulated Brillouin scattering based optoelectronic oscillator," Optical Fiber Technology, **46**, 68 (2018).

[23] X. Zhang, T. Pu, J. Zheng, J. Li, Q. He, G. Wu, J. Zhao, S. Chen, W. Mou, "Simple Optical Frequency Comb Generation Based on the Optoelectronic Oscillator," in 20th International Conference on Optical Communications and Networks, Shenzhen, China, August (2022)

[24] Y. Zhang, B. Yuan, L. Li, J. Zeng, Z. Shang, J. Zheng, Z. Lu, S. Guan, X. Zhang, R. Xiao, T. Fang, Y. Shi, H. Zou, J. Shen and X. Chen, "Experimental demonstration of single sideband modulation utilizing monolithic integrated injection locked DFB laser". J. Lightw. Technol., **38**, 1809 (2020).

[25] Y. Zhang, B. Yuan, L. Li, J. Zeng, Z. Shang, J. Zheng, Z. Lu, S. Guan, X. Zhang, R. Xiao, T. Fang, Y. Shi, H. Zou, J. Shen and X. Chen, "Experimental demonstration of single sideband modulation utilizing monolithic integrated injection locked DFB laser". J. Lightw. Technol., **38**, (2020).